Materials for Energy Technology

MS.4.P104
First high resolution transmission electron microscopy characterization of fcc→9R transformation in nanocrystalline palladium films due to hydriding

B. Aminahmadi[1], H. Idrissi[1,2], R. Delmelle[2], T. Pardoen[2], J. Proost[2], D. Schryvers[1]

[1]University of Antwerp, Physics- Electron microscopy for material science (EMAT), Antwerpen, Belgium
[2]Université catholique de Louvain, Institute of Mechanics, Materials and Civil Engineering, Louvain-la-Neuve, Belgium

behnam.amin-ahmadi@ua.ac.be
Keywords: Nanocrystalline Palladium, ∑3{112} twin boundary, 9R phase

Thin palladium (Pd) membranes constitute an enabling material in hydrogen permeation and sensing applications essential for hydrogen energy technology. These membranes must be as thin as possible to ensure high hydrogen permeability while remaining mechanically stable. It has been recently reported that the ductility of Pd thin films with an average grain size of 30 nm can be significantly improved due to the presence of coherent growth nanotwins [1].

In the present work, nanocrystalline (nc) Pd films with 150 nm thickness containing nanoscale growth ∑3{111} coherent TBs (CTBs) and ∑3{112} incoherent TBs (ITBs) were produced using sputter deposition and subjected to hydriding cycles. Figure 1(a) is a BF image of a plan-view FIB sample of the as-sputtered Pd film. The average in-plane grain size equals 26±1 nm while the cross-sections reveal a columnar morphological texture with an average elongated aspect ratio (height/lateral dimension ratio) of 3. Growth nanotwins are indicated by white arrows in Figure 1(a). In Figure 1(b), a <110> HRTEM image of a single grain is shown in which parallel ∑3{111} CTBs connected by ∑3{112} ITBs are recognized. The incoherent character of the ∑3{112} ITBs can be clearly distinguished in the Geometrical Phase Analysis (GPA) map of Figure 1(c) with an array of misfit dislocations located at the ∑3{112} ITBs. Figure 1(d) shows the evolution of the internal stress as a function of time during a complete hydriding cycle at P_{H2} = 97.5 mbar. This pressure is large enough to induce the α→β transformation in nc Pd. The initial volume of the Pd structure expands by about 10% during this phase transformation [2], which induces a plastic deformation within the Pd film.

After a hydriding/dehydriding cycle of Pd films, it was observed that ∑3{112} ITBs dissociate into two phase boundaries bounding a new and thermodynamically unstable 9R phase with the formation of single stacking faults every three {111} planes. Figure 2(a) shows a <110> oriented HRTEM micrograph of a straight band exhibiting two common {111} interfaces bounding a 9R phase in a hydrided Pd sample. However, care needs to be taken not to confuse a genuine 9R area with an overlapping region between twin and matrix, also causing an extra threefold periodicity in the <110> HRTEM images of an fcc lattice. The difference between both cases can be observed from the actual position of these 1/3 extra spots in the first rows next to the central <111> row. By analysis of the Fast Fourier Transform (FFT) of the HRTEM images, for a true 9R structure, observed along a $<110>_{fcc}$ direction, none of the spots in these rows coincides with the center normal to the <111> long period axis, as seen in the example of Figure 2(a). On the other hand, for the overlapping case, this normal crosses the middle spot in the adjacent row, as seen in Figure 2(b).

The sizes of the observed 9R regions and thus the dissociation width of the ∑3{112} ITBs are in the 5 to 30±1 nm range. Figure 3(b) shows an example of a smaller 9R region after hydriding indicating that not all regions involve extended dissociation. Figure 3(c) exhibits a GPA map of the region indicated by solid lines in Figure 3(b); the misfit dislocations located at the two 9R phase boundaries can be clearly observed. In the area indicated by dashed lines in Figure 3(b), the exact stacking is revealed from the HRTEM lattice micrograph, further enlarged in Figure 3(d) and which exhibits some stacking defects (due to secondary GB dislocations) within the perfect 9R sequence.

This is the first time the 9R structure is reported in nc Pd. This observation is unexpected when considering the high stacking fault energy (SFE) of Pd. This observation is explained by the influence of the hydrogen on the SFE of Pd and the high compressive stresses building up during hydriding.

1. H. Idrissi, B. Wang, M.S. Colla, J.P. Raskin, D. Schryvers and T. Pardoen, Adv. Mater. 23 (2011), P.2119.
2. M. V. Goltsova, and G. I. Zhirov, Met. Sci. Heat Treat. 49 (2007), P.141.
3. J. Wang, A. Misra, and J. P. Hirth, Phys. Rev. B 83, (2011) P. 64106.

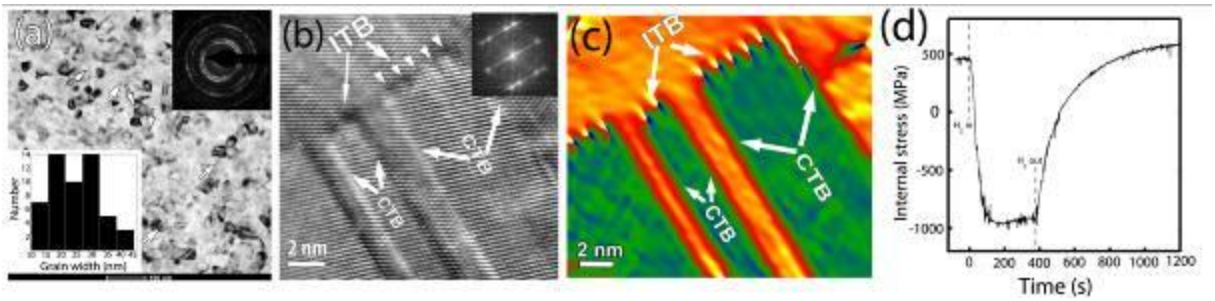

Figure 1. (a) BF micrograph of plan-view FIB specimen prepared from as-deposited Pd film. Growth twins are shown by white arrows. Upper-right inset SADP shows the fcc Pd crystalline structure. Lower-left inset shows the grain width distribution of as-deposited Pd film. (b) HRTEM micrograph of an as-deposited cross-section specimen showing ∑3{111} CTBs and ∑3{112} ITBs. (c) GPA map of the HRTEM image of Figure 1b (d) Evolution of the internal stress as a function of time during a hydriding cycle recorded at P_{H2}=97.5 mbar.

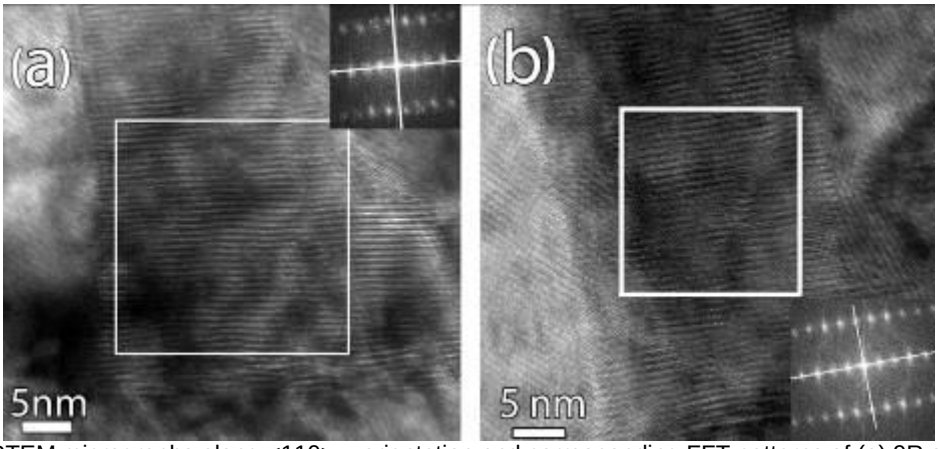

Figure 2. HRTEM micrographs along <110>$_{fcc}$ orientation and corresponding FFT patterns of (a) 9R structure and (b) overlap structure of twin and matrix for Pd thin film after hydriding. The FFT was performed from the regions indicated by white squares.

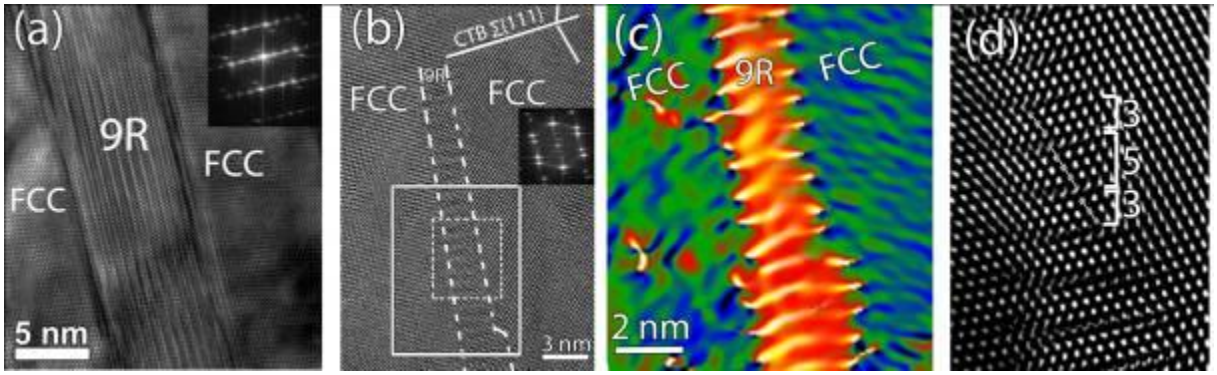

Figure 3. (a) <100> HRTEM image of a 9R band embedded in the fcc Pd matrix after hydriding. (b) <100> HRTEM image of narrowly dissociated ∑3{112} ITBs with the corresponding FFT pattern showing the local 9R structure. (c) collated GPA map of the region indicated by solid lines in the HRTEM image of (b). (d) Enlargement of the region of (b) indicated by dashed lines showing a (defected) atomic stacking sequence of the 9R phase.